

# Assessment of viral and non-viral gene transfer into adult rat brains using HSV-1, calcium phosphate and PEI-based methods

Thomas D. Corso<sup>1, 2</sup>, German Torres<sup>3</sup>, Christopher Goulah<sup>1</sup>, Indrajit Roy<sup>4</sup>, Angelo S. Gambino<sup>1, 2</sup>, John Nayda<sup>2</sup>, Timothy Buckley<sup>2</sup>, Ewa K. Stachowiak<sup>1</sup>, Earl J. Bergey<sup>4</sup>, Haridas Pudavar<sup>4</sup>, Purnendu Dutta<sup>4</sup>, David C. Bloom<sup>5</sup>, William J. Bowers<sup>6</sup>, Michal K. Stachowiak<sup>1, 4</sup>

<sup>1</sup>Molecular and Structural Neurobiology and Gene Therapy Program, University at Buffalo, SUNY, USA

<sup>2</sup>Chemistry and Biochemistry, Canisius College, Buffalo, NY, USA

<sup>3</sup>Department of Neuroscience, NYCOM/NYIT, Old Westbury, New York, USA

<sup>4</sup>Institute of Lasers, Photonics and Biophotonics, University at Buffalo, SUNY, USA

<sup>5</sup>Molecular Genetics & Microbiology, University of Florida College of Medicine, Gainesville, USA

<sup>6</sup>Center for Aging and Developmental Biology, University of Rochester School of Medicine and Dentistry, Rochester, NY, USA

[Received 18 June 2005; Accepted 15 July 2005]

*CNS gene transfer could provide new approaches to the modelling of neurodegenerative diseases and devising potential therapies. One such disorder is Parkinson's disease (PD), in which dysfunction of several different metabolic processes has been implicated. Here we review the literature on gene transfer systems based on herpes simplex virus type 1 (HSV-1) and non-viral polyethyleneimine (PEI) and calcium phosphate nanoparticle methods. We also assess the usefulness of various CNS gene delivery methods and present some of our own data to exemplify such usefulness. Our data result from vectors stereotaxically introduced to the substantia nigra (SN) of adult rats and evaluated 1 week and/or 1 month post injection using histochemical methods to assess recombinant  $\beta$ -galactosidase enzyme activity. Gene transfer using PEI or calcium phosphate-mediated transfections was observed for both methods and PEI was comparable to that of HSV-1 amplicon. Our data show that the amplicon delivery was markedly increased when packaged with a helper virus and was similar to the expression profile achieved with a full-size replication-defective HSV-1 recombinant (8117/43). We also examine whether PEI or HSV-1 amplicon-mediated gene transfer could facilitate assessment of the biological effects induced by a dominant negative FGF receptor-1 mutant to model the reduced FGF signalling thought to occur in Parkinson's disease.*

**Key words:** Parkinson's disease, fibroblast growth factor, *substantia nigra*, gene transfection, herpes simplex virus-1, polyethyleneimine, calcium phosphate nanoparticle, tyrosine kinase, adenovirus,  $\beta$ -galactosidase

## INTRODUCTION

The *in vivo* introduction of genes into the brain and spinal cord is a challenging task, which holds promise for unravelling the functions of specific genes, modelling diseases by delivering “pathological” genes, and also for reversing the detrimental effects of missing or defective genes. Because of this promise, the search for effective and reliable *in vivo* gene transfer techniques is an ongoing endeavour.

Remarkably, the injection of DNA plasmid alone, directly into animal foetuses, has been shown to have a greater than 20% integration and transcription of the reporter gene in the gonad, gut, liver, spleen, lung and brain tissue [20]. Unfortunately, gene transfer into the adult mammalian brain using this method has met with little success. In facilitating this transfection, various chemical and viral methods have proven to varying degrees effective.

Facilitation of gene transfer using cationic liposome-mediated transfection of plasmids containing the *lacZ* gene into the caudate-putamen of adult mice has been reported, with expression lasting at least 21 days post transfection [50]. However, the efficiency of this method for *in vivo* work is low, with typical results showing only several weakly stained cells in the brain region adjacent to the injection site [33].

A similar, but more successful agent is PEI, which is an effective gene transfection agent even in the adult mammalian brain [8]. Every 3<sup>rd</sup> atom in PEI molecule is a protonable amino nitrogen atom, which makes the polymeric association with negatively charged DNA an effective “proton sponge”. This allows for endosome buffering and thus protects DNA from lysosomal degradation. PEI can exist as either a linear or a branched polymer, although the linear PEI of 25 kDa or less seems to be the most effective [1]. One example of this is a report documenting the linear form to be better for transfections into tumours [15]. Another example shows success using linear 22 kDa PEI to transfect neurons and glia adjacent to the ventricular system following intraventricular injections (in mice) [22] and in the xenopus tadpole brain [45]. In the latter case, intraventricular microinjections of 1 microlitre (containing 0.5 to 1 microgram DNA) showed that the linear low molecular weight polymer 22 kDa PEI was significantly more efficient than a branched 25 kDa polymer [45]. In mice intraventricular injections of PEI/DNA with *lacZ* reporter (beta-galactosidase gene) by cre-recombinase to R26R mice demonstrated survival and migration of stem cell derivatives 3 months after injection [36]. The solvent vehicle used for PEI is also im-

portant since the salt-free linear PEI22/DNA is about 10–100 times more effective than the branched PEI/DNA and salt-containing PEI22/DNA complexes [71].

Another well-proven method is the calcium phosphate precipitate method, which has been widely used for *in vitro* transfection, owing to the ability of calcium ions to complex with plasmid DNA as well to form ion-channels in cell membranes [23, 66]. Unfortunately, owing to the bulk size of these complexes and the inadequate protection of plasmid DNA from enzymatic digestion, early experiments *in vivo* did not enjoy great success. However, an improvement on this technique used nanoparticles of calcium phosphate to accomplish both *in vitro* and *in vivo* transfection [51]. This improvement is probably due to the encapsulation of the plasmid DNA; thus protecting it from enzymatic digestion. A very recent report stated that the *in vitro* transfection efficiency of 100–120 nm diameter calcium phosphate nanoparticles was higher than that of commercial transfecting reagents [5]. Finally, recent studies have shown that by functionalising the nanoparticles with appropriate ligands, the system can be targeted to selected cell types *in vivo* [51]. These properties, coupled with the biodegradability of calcium phosphate, prompted us to investigate this system for delivering foreign genes into the brain.

In considering viral methods, Herpes Simplex Virus-1 (HSV-1) is a particularly useful vector for delivering and expressing foreign genes within CNS. This neurotropic virus possesses a complex genetic program that leads to it spending most of its life cycle within the nervous system [58, 68]. HSV-1 enters neurons at the periphery and travels via axonal transport to cell bodies of the sensory ganglia, where it becomes latent [58, 68]. One of the promising HSV-1 vectors is an ICP4-replication deficient virus recombined with a HSV latency-associated transcript promoter (LAT) and the Moloney murine leukemia virus LTR (LAT/LTR) fused with the coding sequence for *E. coli lacZ* gene (ICP4-LAT/MoMuLVLTR/ $\beta$ -gal cassette) [7]. This vector has been shown to transfect both the hippocampus and SN [59].

An alternative and simpler vector platform is HSV-1 amplicon, a drastically minimised derivative of the replication-defective full size recombinant HSV-1 vectors. These vectors are transfected into packaging cells, in which, through complementation with a replication-defective helper virus or a bacterial artificial chromosome carrying a pac-deficient HSV genome, viral particles are assembled [11, 39]. Amplicon vectors have been used previously to deliver nerve

growth factor (NGF) to mice that were heterozygous for a null NGF gene (*ngf*(+/-)) and it was found that improvements in spatial learning could be quantified [13]. HSV amplicon-mediated transductions have been used to deliver genes such as neurotrophin-3 to protect murine spiral ganglion neurons from cisplatin-induced damage both *in vitro* [14] and *in vivo* [9]. HSV-1 amplicons have also been used for gene therapy of malignancies and it has been shown that helper virus-free HSV-1 amplicon preparations are better suited for immunotherapy [62, 63, 72] and leukaemia [61]. Other uses of this viral-based gene delivery method have included glucocorticoid-regulated VEGF expression [24] and human immunodeficiency virus type 1 gp120 expression [27, 70]. Immunological responses to this HSV-1 vector have been described [12] and vectors that are helper virus-free trigger a much diminished response [44].

Given the interest in developing new models as well as treatments for diseases such as PD, the experiments used here involved inoculation of the viruses or the direct injection of plasmids into the dopamine (DA) producing SN area. In the present study we utilised 4 different intra-brain gene transfer methods, employing two HSV-1 derived vectors and two plasmid transfection techniques. The efficacy of different gene transfer protocols was evaluated using *lacZ* as the reporter gene. The effectiveness of the non-viral polyethyleneimine (PEI) protocol and the amplicon viral method was also confirmed by transfecting a mutant gene coding for FGFR1(TK-) [48] and then showing its effects on neuronal survival.

Our interest in the FGFR1 stems from work by Tooyama et al. [64], who found that in all PD patients examined the content of the primary growth factor that binds the FGFR1, fibroblast growth factor-2 (FGF-2), becomes depleted prior to cell degeneration in SN DA neurons. FGF-2 depletion was not observed in aged non-Parkinsonian individuals [65], indicating that FGF-2 defect is specifically associated with PD. Even though there may not be a reduction in the content of the FGF receptors, including FGFR1 [69], there could still be a disruption of the signalling produced by this receptor. Therefore, FGFR1 receptor disruption in SN of Parkinsonian patients could play a role in the loss of DA neurons associated with that disease.

In order to inhibit the FGF signalling, we have been using a dominant negative receptor mutant of fibroblast growth factor type 1 with a deleted tyrosine kinase domain [FGFR1(TK-)], which forms non-

functional heterodimers with any of 3 FGFR1-3, thus eliminating the signalling by the wild type FGFR's [67]. *In vitro*, we found in rat sympathetic neurons that PEI-transfected FGFR1(TK-) inhibited bone morphogenetic protein-7 (BMP-7) induced dendritic growth [28, 29] and cAMP-induced axonal outgrowth in human neuronal precursor cells [54, 56]. In glioma FGFR1(TK-) inhibited cell proliferation [55, 56]. *In vivo* we tested the hypothesis that diminished FGF signalling may be a contributing factor in the etiology of PD and showed that transfection of the FGFR1(TK-) can decrease the number of TH-positive neurons in SN and the concentration of DA in the striatum of rats (manuscript in press) [17].

Here we show our data for 2 HSV-1 viral methods and for PEI and calcium phosphate nanoparticle methods. In addition, we also show the effect of FGFR1(TK-) transfection on SN cells.

## MATERIAL AND METHODS

### Plasmids

pcDNA3.1-FGFR1(TK-) expressing FGF receptor-1 with deleted tyrosine kinase domain and pCMVpcMV- $\beta$ -gal expressing  $\beta$ -galactosidase cDNA from the cytomegalovirus (CMV) late promoter have been described previously [48, 49, 54]. The plasmids were isolated and purified using a QIAGEN (Valencia, CA) endotoxin-free kit.

### Preparation of PEI

PEI/DNA complexes were prepared using ExGen 500, (MBI Fermentas Inc.), a cationic linear PEI polymer. Freshly prepared mixtures of plasmid DNA and PEI dissolved in 5% glucose were used. These consisted of 3–5  $\mu$ l containing 1.5–3.0  $\mu$ g of plasmid DNA and 6 PEI equivalents of DNA (one equivalence = amount of PEI required to neutralise the negative charges of DNA phosphate groups).

The complexation of PEI with plasmid DNA was carried out in 2 stages, using sterile chemicals in a sterile chamber. In the first stage, plasmid DNAs (pCMV- $\beta$ -gal and pcDNAFGFR1(TK-)) of known concentrations were mixed with 15% aqueous dextrose solution and water to get a final DNA concentration of 0.6 mg/ml. After brief vortexing and centrifugation, the solutions were kept on ice for 12 hours. In the second stage, carried out just before surgery, 25  $\mu$ l of the 0.6 mg/ml DNA solutions were mixed with 2.7  $\mu$ l and 3.6  $\mu$ l of ExGen500 PEI solutions to obtain PEI-DNA complexes of 6 and 8 equivalents, respectively. The final dextrose concentration in the

solutions was 5%. After brief vortexing and centrifugation, the solutions were kept at room temperature for 10 min prior to injection in the rat brain.

### Preparation of the calcium phosphate nanoparticles

Sodium bis(ethylhexyl) sulphasuccinate (AOT) of 0.1 M in hexane was prepared. In 25 ml of AOT in hexane 50 ml of aqueous solution of  $\text{CaCl}_2$  (20% w/v), 400 ml of double distilled water and 10 mg of plasmid DNA were dissolved by continuous stirring for 72 h to form a microemulsion A. In another 25 ml of AOT in hexane 50 ml of aqueous solution of  $\text{Na}_2\text{HPO}_4$  (5% w/v), 350 ml of double distilled water, 50 ml of 0.2 M Tris-HCl buffer (pH 6) and 10 ml of plasmid DNA were dissolved by continuous stirring for 48 h to form a microemulsion B. Both the microemulsions were optically clear solutions. Microemulsion B was then slowly added to microemulsion A at 5 ml/h with continuous stirring at 8–10°C. The resulting solution was then further stirred for another 6 h, after which it was centrifuged at  $8 \times 10^3$  rpm for 30 min. The pelleted nanoparticles were washed with hexane 3 times and finally redispersed in 10 ml of double distilled water by sonication (frequency 22 kHz, power 120 W) for 2 h. The dispersed nanoparticles were dialysed for 10 h and were kept at –4°C for further use.

### Preparation of the amplicon virus

**Cell culture.** Neonatal hamster kidney (BHK) and RR1 cell lines were maintained as previously described [38]. The NIH-3T3 mouse fibroblast cell line was originally obtained from American Type Culture Collection and maintained in Dulbecco's modified Eagle medium with the addition of 10% foetal bovine serum.

**Amplicon construction.** The coding sequence for *E. coli*  $\beta$ -galactosidase was cloned into an HSV amplicon plasmid vector as previously described [21].

**Helper virus-based amplicon packaging.** Amplicon DNA was packaged into HSV-1 particles by transfecting 5  $\mu\text{g}$  of plasmid DNA into RR1 cells with Lipofectamine as recommended by the manufacturer (Gibco-BRL). Following incubation for 24 h, the transfected monolayer was superinfected with the HSV strain 17-derived IE3 deletion mutant virus D30EBA [46] at a multiplicity of infection (MOI) of 0.2. Once cytopathic changes were observed in the infected monolayer, the cells were harvested, freeze-thawed, and sonicated using a cup sonicator (Misonix, Inc.). Viral supernatants were clarified by centrifugation at  $5,000 \times g$  for 10 min prior to repeat passage on RR1 cells. This second viral passage was

harvested as above and frozen. The frozen virus samples were thawed on ice and sonicated on ice 3 times in a cup sonicator for 30 s. The sample was centrifuged twice at  $2000 \times g$  for 10 min to pellet cellular debris and the supernatant was retained. The clarified viral supernatant was then applied to the top of the 30% layer of a 30%/60% discontinuous sucrose gradient and centrifuged at  $106,000 \times g$  at 4°C for 1 h. The viral band appearing at the interface between the 30% and 60% layers was carefully extracted. The virus was subsequently concentrated via centrifugation through a 30% sucrose cushion at  $106,000 \times g$  at 4°C for 30 min. Viral pellets were resuspended in PBS ( $\text{Ca}^{2+}$  and  $\text{Mg}^{2+}$  free) and stored at –80°C for future use. HSV-1 amplicon expression titer was  $8.03 \times 10^7$  blue-forming units per ml (bfu/ml) and the helper virus titer was  $3.6 \times 10^7$  plaque-forming units per ml (pfu/ml) as determined by X-gal histochemistry on transduced NIH 3T3 cells and plaque-forming assays on transduced RR1 cells. The frequency of wild-type virus reversion was determined to be 1 in  $10^6$  pfu as examined by plaque assays on the non-complementing Vero cell line.

### Helper virus-free amplicon packaging (HF-HSV).

Amplicon stocks were also prepared using a modified helper virus-free packaging method [10]. The packaging system utilises a bacterial artificial chromosome (BAC; kindly provided by C. Strathdee) that contains HSV genome without its cognate packaging (pac) signals as a co-transfection reagent with amplicon DNA. Because the amplicon vector possesses a pac signal, only the amplicon genome can be packaged. Briefly, on the day prior to transfection  $2 \times 10^7$  BHK cells were seeded in a T-150 flask and incubated overnight at 37°C. On the day of transfection, 1.8 ml Opti-MEM (Gibco-BRL), 25  $\mu\text{g}$  of pBAC-V2 DNA [57], 7  $\mu\text{g}$  of pBS(vhs), and 7  $\mu\text{g}$  amplicon vector DNA were combined in a sterile polypropylene tube. Over a period of 30 s 70 ml of Lipofectamine Plus Reagent (Gibco-BRL) was added to DNA mix and allowed to incubate at 22°C for 20 min. In a separate tube 100  $\mu\text{l}$  Lipofectamine (Gibco-BRL) was mixed with 1.8 ml Opti-MEM and also incubated at 22°C for 20 min. Following the incubations, the contents of the 2 tubes were combined over a period of 30 s and incubated for an additional 20 min at 22°C. During this second incubation the media in the seeded T-150 flask was removed and replaced with 14 ml Opti-MEM. The transfection mix was added to the flask and allowed to incubate at 37°C for 5 h. The transfection mix was then diluted with an equal volume of DMEM plus 20% FBS and 2 mM hexame-

thylene bis-acetamide (HMBA) and incubated overnight at 34°C. On the following day the medium was removed and replaced with DMEM plus 10% FBS and 2 mM HMBA. The packaging flask was incubated for an additional 3 days before the virus was harvested and stored at -80°C until purification. Viral preparations were subsequently purified and concentrated as for helper virus-containing stocks. Expression titers were determined by enumeration of X-gal-positive NIH 3T3 cells transduced with serial dilutions of amplicon stocks. Wild-type reversion frequency was found to be less than 1 in 10<sup>7</sup> expressing amplicon particles as determined by plaque assay on transduced Vero cells.

#### Preparation of the amplicon containing FGFR1(TK-)

FGFR1(TK-) cDNA with deleted tyrosine kinase region (TK) was cloned into pHSVPrPUC parent amplicon plasmid using standard procedures. Helper virus-free HSV FGFR1(TK-) amplicon stocks were prepared as described above.

#### Preparation of HSV-1 8117/43 and KD6

The HSV 8117/43 construct utilised in this experiment was created by deleting the ICP4 gene from the non-replicating HSV vector and inserting the Mouse Moloney Leukemia virus (MoMuLV) long terminal region (LTR) promoter, a gene essential for replication, which is a transcription unit that replaces both copies of the ICP4 gene [19, 40, 53]. Briefly, the construct 8117/43 contains the *E. coli lacZ* reporter gene driven by the MoMuLV LTR in place of the deleted ICP4. It also has a 2.3 kb BstEII deletion in the LAT (latency associated transcript) promoter region. The control construct, KD6, contains the same deletion but lacks the *lacZ* insert. Both KD6 and 8117/43 were propagated on the E5-complementing cell line, a generous gift of N. DeLuca. Infected cells were harvested and concentrated by centrifugation at 10,000 × g (30 min at 4°C) and resuspended in 1/100 of the original cell culture volume in MEM with 10% FBS. Vector was released from the infected cells and subjected to 2 rounds of freeze-thawing. The stocks were clarified by centrifugation for 2 min at 10,000 × g, and the supernatant aliquoted and frozen at -80°C. Stocks were titrated on complementing E5 cells and the number of ICP4(+) revertants determined by passage and titration on RS cells (non-permissive for ICP4(-)). All stocks used in this study had < 1 revertant per 1 × 10<sup>6</sup> PFU of ICP4(-) plaques, as determined by differential analyses on E5 (com-

plementing) vs. RS (non-complementing cell lines). The amounts of virus used in specific experiments are shown in the captions to the figures.

#### Animals

Adult Male Fischer 344 rats (Harlan Sprague-Dawley Inc., NIA colony) with an average body weight of 180–250 g were used. The animals were housed in the Laboratory Animal Facilities in the School of Medicine and Biomedical Sciences at the State University of New York at Buffalo. The rats were anaesthetised with a mixture of ketamine (100 mg/ml), xylazine (20 mg/ml), and ace-promazine (10 mg/ml) in 0.9% NaCl (0.2 ml/100 g body weight, i.p.) placed in stereotaxic apparatus and received unilateral or bilateral injections (depending on the experiment) into the SN region of the brain at the co-ordinates of -5.6 mm (posterior), ± 1.5 mm (lateral), -8.2 mm (ventral) from the bregma [47]. Each injection delivered 3 to 5 µl of solution to each site at a rate of 0.5 µl/min by means of a 30 G stainless steel needle on a 10 µl Hamilton syringe held by the micromanipulator on the stereotaxic apparatus. The needle was slowly removed 5 min after the completion of the injection. The wound was then sutured. All procedures were approved by the Institutional Animal Care and Use Committee guidelines (IACUC) of the State University of New York at Buffalo. For HSV-1 (8117/43) injections 4 µl containing 2 × 10<sup>6</sup> plaque-forming units (pfu) was injected per site. For the amplicon helper-free 1.92 × 10<sup>5</sup> pfu/4 ml was injected. For HSV-1 amplicon (1.3 × 10<sup>5</sup> pfu/4 ml) containing the helper virus, 1.4 × 10<sup>5</sup> pfu/4 ml was injected.

#### Tissue preparation and histochemical detection of β-galactosidase activity

The rats were deeply anaesthetised (as described above for surgery) and were perfused transcidentally with PBS (pH 7.4) followed immediately by ice-cold fresh 4% paraformaldehyde fixative in 0.2 M phosphate-buffer (pH 7.4). The brains were removed, placed in the paraformaldehyde fixative solution then cut into 2-mm coronal sections using a stainless steel brain mould. These sections were post-fixed with 2% formaldehyde, 0.2% glutaraldehyde, 0.01% NaDOC (sodium deoxycholate) and 0.02% NP-40 for 1 h at 4°C. The tissue was then washed twice with PBS followed by 3% DMSO/PBS. The X-gal staining solution consisted of 0.87 g NaCl, 100 mM HEPES, pH 7.5, 2 mM MgCl<sub>2</sub>, 0.01% NaDOC, 0.02% NP-40, 5 mM potassium ferricyanide and 5 mM potassium ferrocyanide. This solution was freshly prepared and kept

at 4°C. When ready to use, the solution was warmed to 36°C and 5 ml of 2% X-gal [5-bromo-4-chloro-3-indolyl  $\beta$ -D-galactopyranoside] in dimethyl formamide were added. The tissue sections were stained with X-gal for 7 h at 31°C in the dark. Subsequently the slices were washed several times in PBS and placed in 30% sucrose in PBS. All solutions were prepared fresh and their pH was adjusted to 7.3 in order to prevent the detection of endogenous (acidic)  $\beta$ -galactosidase. Sections were photographed either with a digital camera or laid on transparency film and scanned at high resolution.

Following photography, tissues were cryoprotected with 20% sucrose and then further cut into 50- $\mu$ m sections using a freezing stage microtome. Brain sections were mounted onto glass slides, counterstained with Eosin Y, dehydrated and coverslipped. Sections were photographed on an Edge 400 microscope.

#### Tyrosine hydroxylase (TH) immunostaining

Tissue staining was performed using rabbit anti-TH antibody (Chemicon, cat#AB151). Sections were pre-incubated in a blocking solution of 10% bovine serum albumin (BSA) in PBS for 50 min at room temperature and incubated in anti-mouse primary antibody (1000:1) overnight in 1% BSA in PBS at 4°C. Sections were then washed 3 times at 2 min per wash with PBS to remove primary antibody, and incubated in biotinylated anti-rabbit secondary antibody at a 100:1 ratio for 50 min at room temperature in a 1% BSA in PBS and washed 3 times at 2 min per wash. The sections were then washed in 3% hydrogen peroxide for 5 min and PBS, again 3 times at 2 min. The sections were then incubated with extra avidin-HRP (ABC) for 50 min at a 100:1 ratio at room temperature in 1% BSA in PBS followed by 2 washes with PBS and 2 with dH<sub>2</sub>O at 2 min per wash. Staining was completed with diaminobenzidine (DAB) for 2 to 5 min until stains appeared followed by 2 washes with distilled H<sub>2</sub>O and 2 with PBS at 2 min per wash. In some cases nickel intensification was used. Following completion of the staining procedures, sections were mounted on slides and coverslipped for examination using a light microscope.

#### Cell size measurements

During the cutting and mounting of the brain sections (in the coronal plane), the right side of the brain was marked by punching a small needle hole through a part of the brain distant to SN (such as the cortex and upper right midbrain area). Each section of the brain was kept and systemically stored.

Every 5<sup>th</sup> section was stained and mounted in sequential order. The level of each section was evaluated using the co-ordinates from Paxinos and Watson [47].

Digital photomicroscopy was used to capture representative regions of SN of 50- $\mu$ m-thick brain sections that were stained with tyrosine hydroxylase immunostaining. A section closest to -5.6 mm AP was chosen, since this is the approximate location of the injection. The microscope was focused on the area of the SNpc closest to the injection co-ordinates of  $\pm$  1.5 mm LM, -5.6 mm AP and -8.2 mm DV and the areas of the 5 closest cells were measured using NIH shareware program Image J. This was done for the left and right side of the same brain section. Since tissue sections can differ in size from each other as a result of varying degrees of shrinkage following staining, processing and dehydration, the average area on the experimental side was divided by the control (or non-injected) side and expresses as a percentage.

## RESULTS

Injection of the *lacZ* reporter gene ( $\beta$ -galactosidase) into SN was employed to visualise the transfection. The X-gal staining procedure detects expressed  $\beta$ -galactosidase activity when the  $\beta$ -galactosidase enzyme cleaves the X-gal substrate into a blue product molecule that precipitates onto the tissue. No staining was observed in controls injected with glucose at 1 week (Fig. 1A, panel I) or 1 month (not shown), although expression of the transfected genes was seen with the full size 8117/43 HSV-1 inoculated into rat brains, resulting in modest staining in the ventral midbrain region 1 week post injection (Fig. 1A, panel II) and strong staining 1 month post injection (Fig. 1A, panel III). Figure 1B shows photomicrographs of staining in SN in 50- $\mu$ m-thick sections. One week following inoculation with control HSV-1 (KD6) lacking the *lacZ* reporter gene, no  $\beta$ -galactosidase activity was detected (Fig. 1B, panel I), whereas 1 week following inoculation with the *lacZ*-containing recombinant (8117/43) we observed a number of cells expressing  $\beta$ -galactosidase activity (Fig. 1B, panel II). An enlarged view of a typical X-gal-positive neuron in the *zona compacta* of SN is depicted (Fig. 1B, panel III). It is important to note that no  $\beta$ -gal expressing cells with astrocytic morphology were observed. Interestingly, over time the expression of  $\beta$ -galactosidase activity increased, and 1 month after inoculation, a greater number of cells showed strong  $\beta$ -galactosidase activity

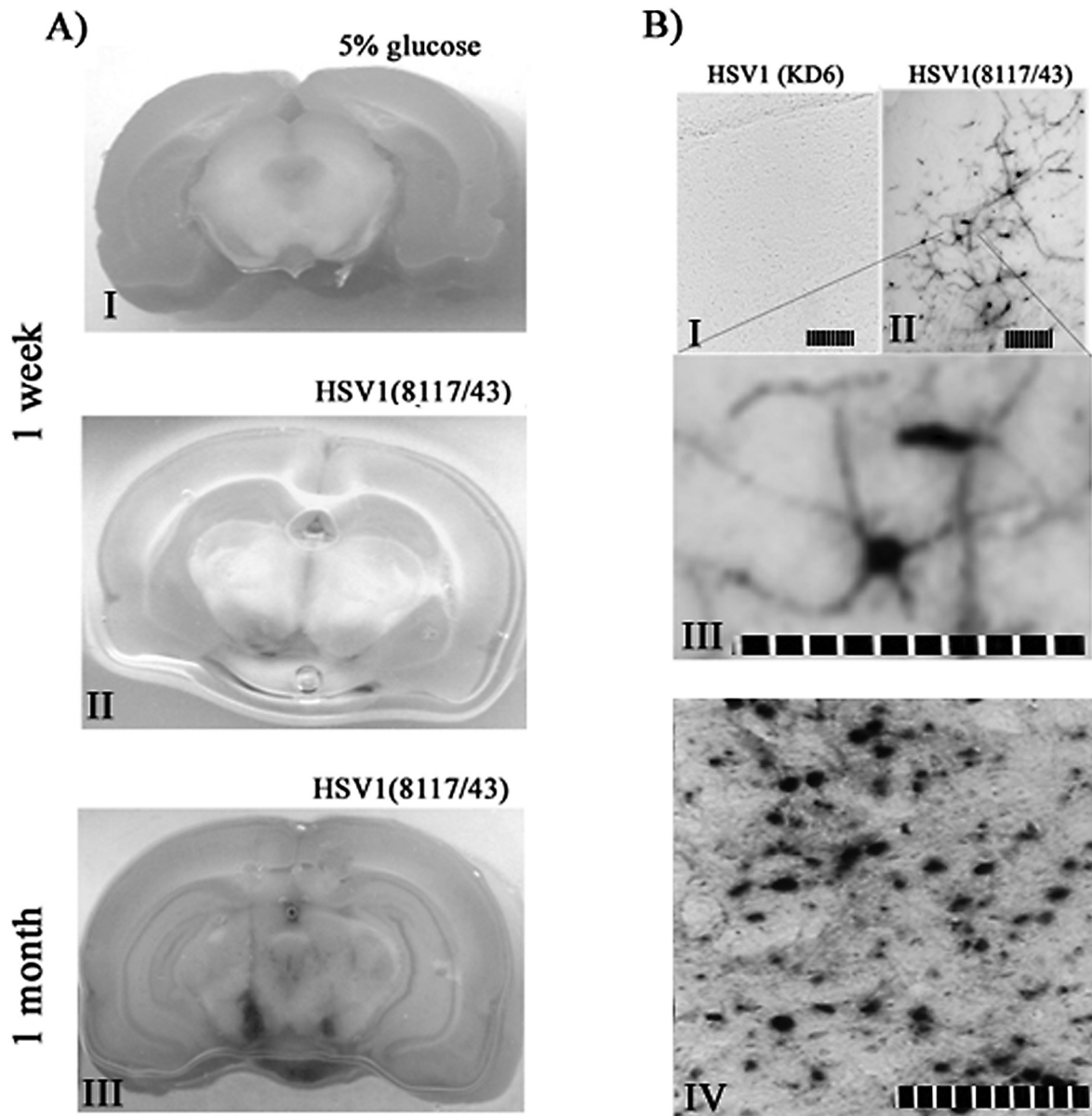


**Figure 1.** Brains of 3-month-old male Sprague-Dawley rats inoculated with HSV-1 (8117/43) [4  $\mu$ l,  $2 \times 10^6$  plaque forming units (pfu) per injection site]. **A.** X-gal staining of 2-mm-thick coronal slabs of rat midbrain 1 week following bilateral injections of 5% dextrose (panel I), 1 week following bilateral injections of HSV-1 8117/43 vector expressing  $\beta$ -galactosidase (middle photograph), and 1 month following bilateral injections of the same virus. The 1 month time point showed the greatest level of expression. **B.** Photomicrographs of X-gal stained 50-mm rat midbrain sections are shown. One week after inoculation of control KD6 HSV1 [(I) tissue was counterstained with eosin to visualise the cells] or  $\beta$ -galactosidase expressing 8117/43 HSV-1 (II). An enlarged 8117/43 HSV-1 infected SN neuron is shown (III). One month post infection of 8117/43 HSV-1 (IV). The scale bar represents 100  $\mu$ m.

(Fig. 1B, panel IV). On the basis of these results we conclude that HSV-1 ICP4(-) vector can be used effectively to express a recombinant gene within the rat SN.

An attractive alternative to the full size virus is the HSV-1 amplicon, which is a minimised derivative of the full size HSV-1, owing to the fact that it may potentially have less of a toxic effect on cells. HSV-1 amplicon-mediated  $\beta$ -galactosidase gene transfer into SN region is illustrated in Figure 2. At the

1 week post-injection time point only minimal X-gal staining was visible on 2-mm tissue slabs (previously published, not shown here) [17], although the use of a "helper virus" significantly increased the level of staining. After only 1 week, even in the gross sections, significant staining is evident (panels I and II). This result was not surprising as the titers of the helper virus-packaged amplicon stocks are typically 10-fold higher than the helper-free stocks. Panel III

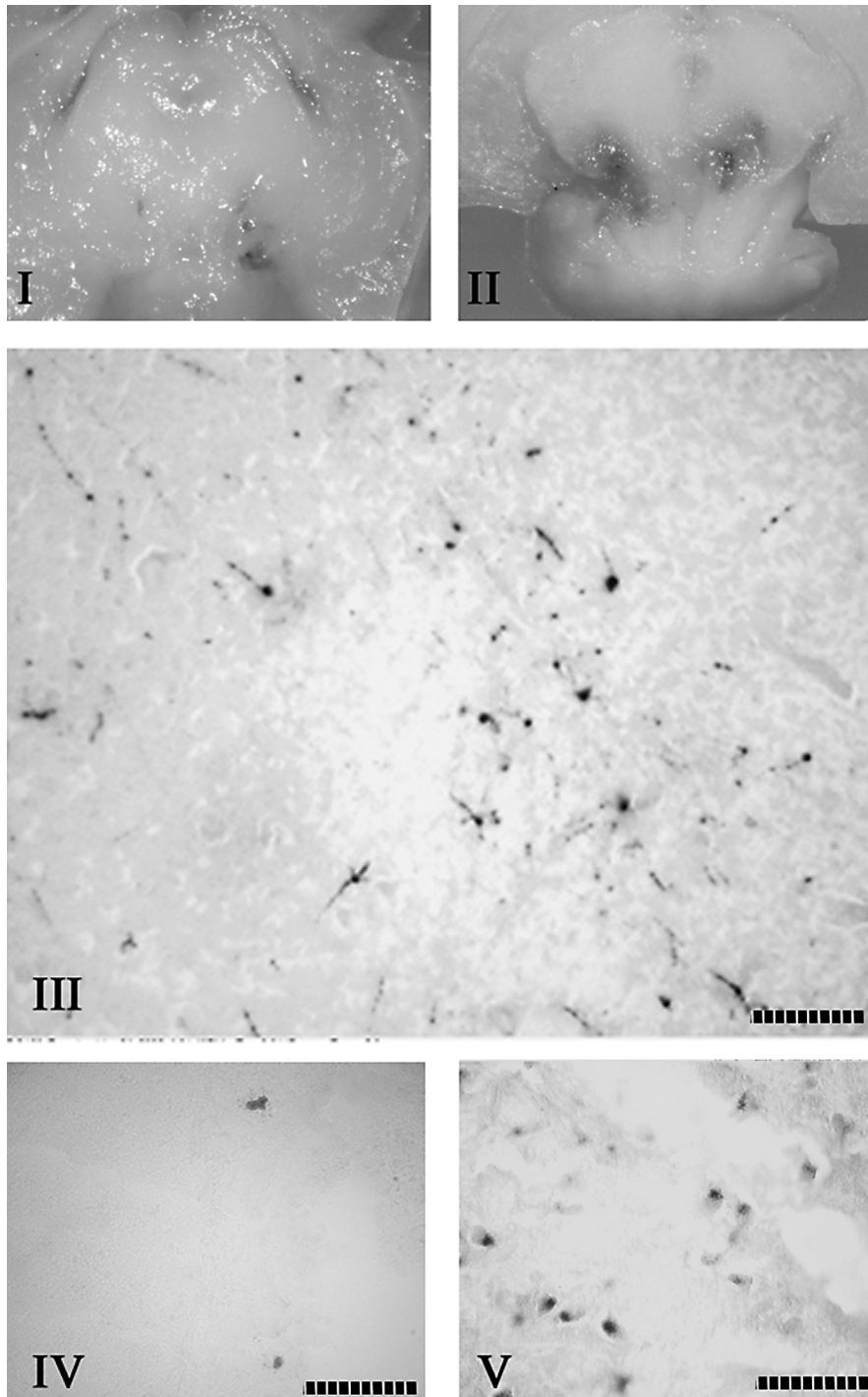


**Figure 2.** Brains of rats inoculated with amplicon vector with helper virus (panels I, II and III) and without helper virus (panels IV and V). Inoculation of HSV-1 amplicon ( $1.3 \times 10^5$  pfu/4  $\mu$ l) containing the helper virus ( $1.4 \times 10^5$  pfu/4  $\mu$ l). At 1 week post inoculation the expression of  $\beta$ -gal activity was visible on 2-mm tissue slabs. Panel I shows injections (from left to right) of 1 and 2 ml and panel II, 3 and 4  $\mu$ l of viral solution. Panel III shows a high magnification photomicrograph of infected SN cells with typical neuronal morphology on a 50- $\mu$ m section. Panels IV and V show helper-free amplicon HSV-1 virus inoculation ( $1.92 \times 10^5$  pfu/4  $\mu$ l) at 1 week post inoculation (panel IV) and 1 month post inoculation (Panel V) on 50- $\mu$ m sections. Minimal staining was seen at 1 week (panel IV) but significant  $\beta$ -gal staining was detected after 1 month (panel V). The scale bar represents 100  $\mu$ m. Panels IV and V are derived from [16] with kind permission from Molecular Brain Research (Elsevier).

shows the typical neuronal morphology of SN cells expressing  $\beta$ -galactosidase activity. In contrast, without the helper virus, there is only minimal staining

1 week following injection (panel IV), although 1 month post inoculation, obvious and significant X-gal staining was observed both on 2-mm tissue



slabs (not shown) and 50- $\mu$ m sections in the area adjacent to the injection site (panel IV).

We also explored 2 non-viral methods. The first was the calcium phosphate nanoparticle method. Calcium phosphate nanoparticle pCMV transfection did not result in detectable  $\beta$ -galactosidase activity 1 week after transfection ( $n = 3$ ) (Fig. 3, panel I). However, in rats that were sacrificed 1 month after transfection we observed an unambiguous X-gal staining in 3 of the 4 rats injected (panel II). The high magnification of the 50- $\mu$ m-thick sections (counterstained with eosin) clearly shows definite profiles of transfected cells (panels III and IV). Interestingly, the stained cells are not in the target SN cells but in the adjacent red nucleus area. The reason for the selective transfection of these cells is not clear at this time.

Our studies with *in vivo* PEI-transfected pCMV $\beta$ -gal plasmid showed the recombinant  $\beta$ -galactosidase activity both at the 1 week (Fig. 4, panels I, II and III) and 1 month time points (Fig. 4, panel IV), although the stain was not as robust as that seen with HSV1 8117/43 vector. The majority of  $\beta$ -galactosi-

dase expressing cells, such as those detected in SN region (panel III) as well as in the more dorsal periaqueductal grey matter (panel I), had a neuronal-like morphology, although a few had an astrocyte-shaped morphology, as seen in Figure 4, panel II. Again, at 1 month, a greater number of cells in SN appear to be positively stained (Fig. 4, panel IV). Overall, using PEI, our studies showed variability between animals, with some transfected predominantly in cells adjacent to the injection sites, while others had much higher levels of  $\beta$ -galactosidase activity with a broader distribution in SN region.

On the basis of the above information, we used 2 of these 4 methods to deliver the defective FGFR1(TK-) gene *in vivo*. Tooyama previously observed a decrease in fibroblast growth factor-2 (FGF-2) in SN-DA neurons prior to cell degeneration in all Parkinson's patients examined [64]. We hypothesised, therefore, that decreased signalling by FGF-2's main receptor, FGFR1, might play a role in the neuronal degeneration observed in PD. As a test of this hypothesis, we delivered the dominant negative

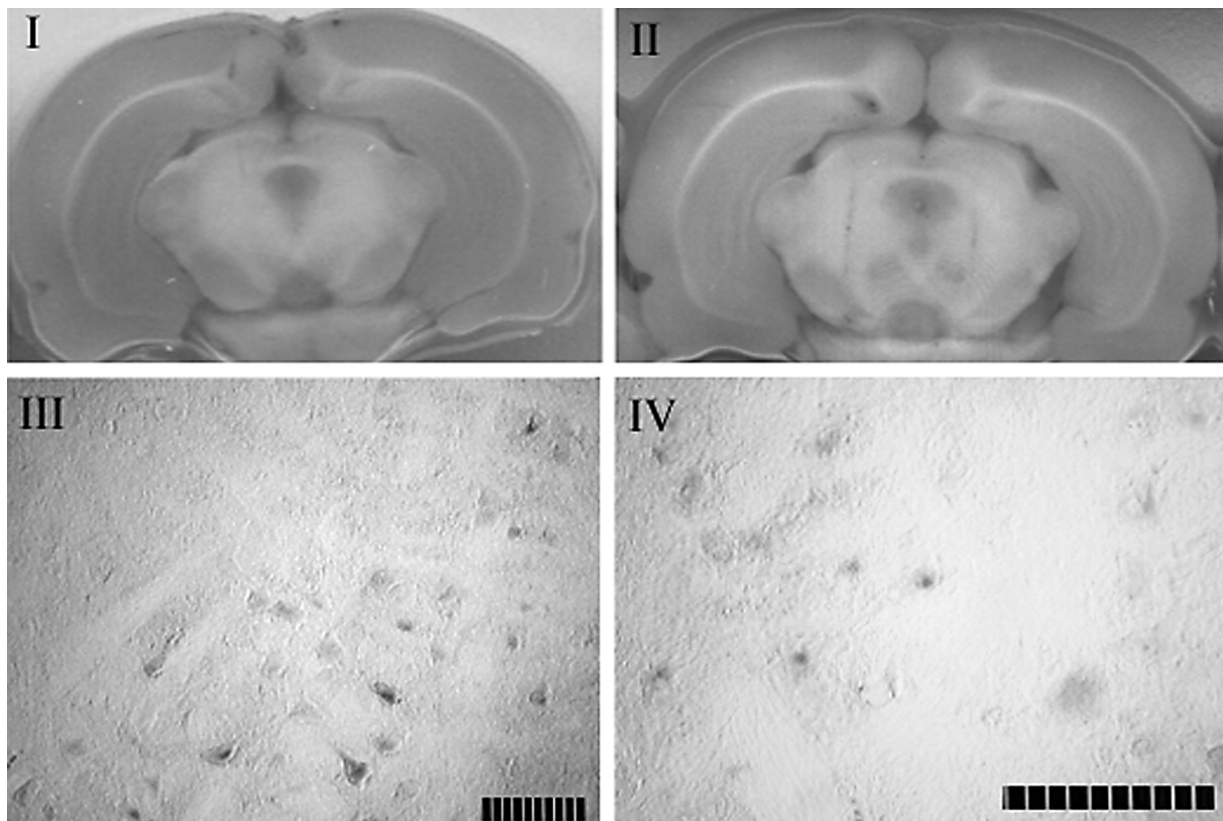


**Figure 3.** Transfection of pCMV-bgal using calcium phosphate nanoparticles. Rats injected with 4  $\mu$ l of calcium phosphate nanoparticles/pCMV- $\beta$ -gal per SN site. One week post transfection no staining was observed — 2-mm tissue slab (I). 1 month post transfection — representative 50-um whole brain section (II) shows  $\beta$ -gal activity in the area of the red nuclei typical for calcium phosphate nanoparticle transfection. III and IV high magnification photographs of cells in the red nuclei areas on both sides of the brain. The scale bar represents 100  $\mu$ m.

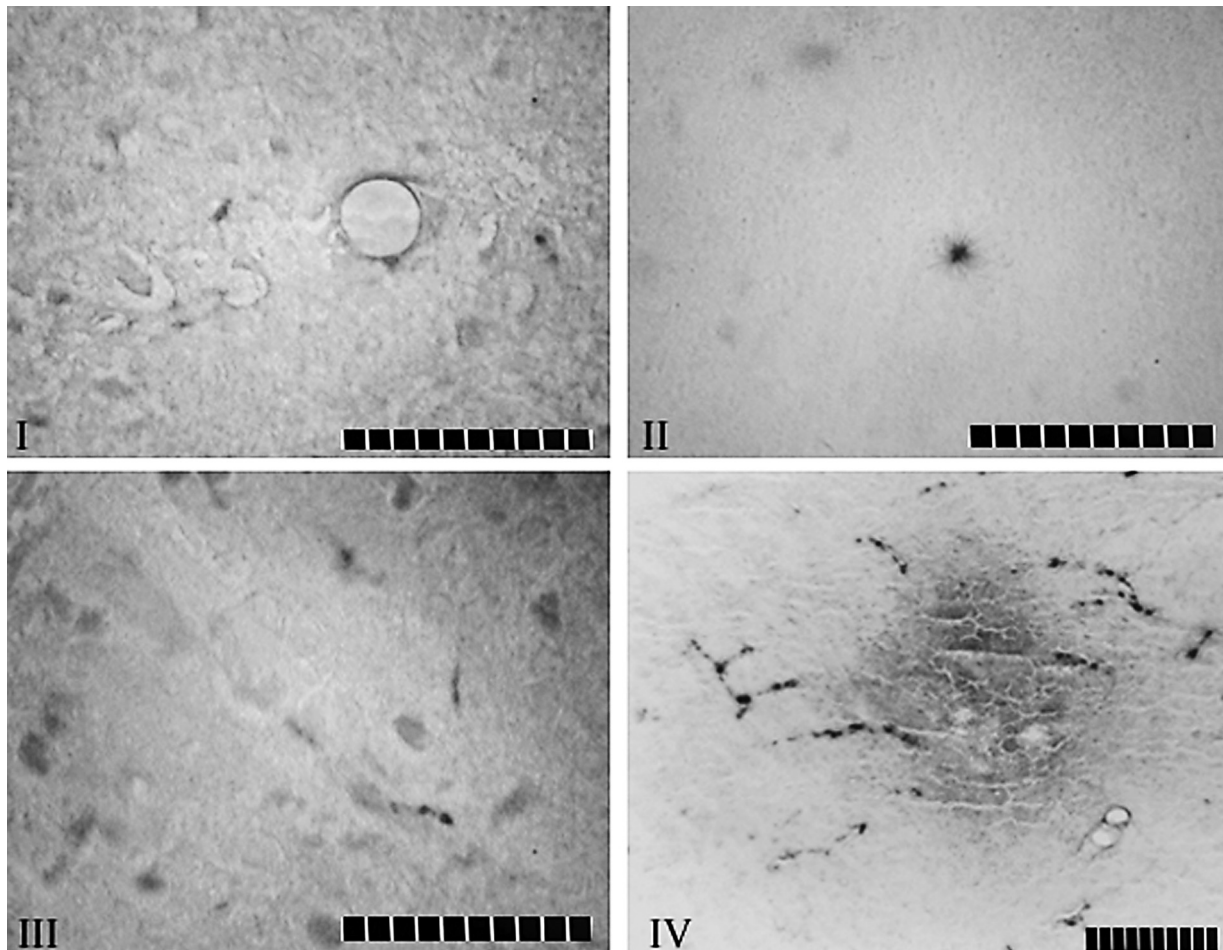


**Figure 4.** PEI-mediated transfection of pCMV  $\beta$ -gal. Rats transfected with 4  $\mu$ l of PEI/ $\beta$ -gal and PEI/pcDNA into the SN area. One week post injection: 50- $\mu$ m midbrain sections showing  $\beta$ -gal expressing cells in periaqueductal grey (I), astrocyte-shaped cell in ventral mid-brain (II) and neuronal-like cells in *substantia nigra* area (III). One month after transfection: the relatively large number of cells shows  $\beta$ -gal activity in the *substantia nigra* (IV). The scale bar represents 100  $\mu$ m. Panels III and IV were derived from [16] with kind permission from Molecular Brain Research (Elsevier).

FGFR1 mutant, FGFR1(TK-), which lacks the tyrosine kinase domain [48, 49]. The non-viral PEI was used but the calcium phosphate method needed more development, since it did not target SN. Both of the viral methods worked well, although we used the amplicon rather than the full size 8117/43 HSV-1 as it allowed faster construction of FGFR1(TK-)-expressing virus.

Figure 5 shows that a decreased number of TH-positive cells can be seen on FGFR1(TK-) injected side. We observed a similar result using the helper-free HSV-1 amplicon as a FGFR1(TK-) DNA delivery vector and have previously reported a statistically significant difference [17].

To ascertain how viral transfection affected cell size; we performed cell area measurements for cells

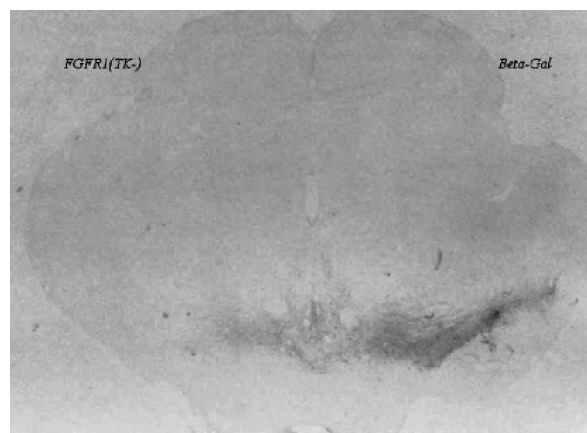


**Figure 5.** The effect of the FGFR1(TK-) delivered by PEI. There are fewer cells on the FGFR1(TK-) side as compared to the control ( $\beta$ -galactosidase) side. The scale bar represents 100  $\mu$ m.

**Table 1.** Average size of cells

	Non-injected side of $\beta$ -galactosidase side	$\beta$ -galactosidase injected side	Non-injected side of FGFR1(TK-)	FGFR1(TK-) injected side of
Average cell area measurements (pixels)	6540.04 $\pm$ 554.76	7003.76 $\pm$ 1202.16	7645.63 $\pm$ 508.56	8438.367 $\pm$ 549.68
Change relative to non-injected side		107.09%		110.37%
The average of the relative percentage for each animal		106.37 $\pm$ 9.66%		110.58 $\pm$ 3.41%

near the injection site. Rats were injected unilaterally with the *lacZ*-containing amplicon virus or with FGFR1(TK-). The average cross-sectional area of TH-positive cells in the SN on the virus-injected side had an area of 106.37  $\pm$  9.66% relative to its non-injected side. FGFR1(TK-) injected side had an average area of 110.58  $\pm$  3.41% relative to its non-injected side. Table 1 below shows our data.

The comparisons were calculated in 2 ways. The first method was to simply average all of the area measurements for each group. These numbers can be seen in the 2<sup>nd</sup> row of the table. The area of the injected side divided by the non-injected side is shown in the 3<sup>rd</sup> row.

The second method for calculating the data was to divide the injected side by the non-injected side for each microscope slide. The number shown in the 4<sup>th</sup> row is the average of all these ratios. This method would negate any variability caused by the shrinkage of the tissue on the microscope slide during mounting and dehydration with alcohol and xylene. As seen, there was virtually no difference in the final results.

## DISCUSSION

The studies presented here have explored the effectiveness of transfecting reporter genes with different viral and non-viral methods. Our studies have shown that all 4 methods discussed here were capable of expressing the *lacZ* reporter gene effectively in the adult rat brain. While at this stage viral vectors appear more efficacious than the non-viral methods used in our study, there are problems inherent in viral transduction, such as potential immune responses and pathologies, especially when the immune system is impaired. Since PEI and, especially, calcium nanoparticles appear to be effective alternatives, further development of these non-viral methods is warranted.

The novel method that we describe here for gene transfection employs calcium phosphate nanoparticles [51]. We show evidence of *in vivo* transfections

into the rat brain in general (Fig. 3), although the staining is not in the target area of SN but rather in the red nucleus. Future modifications of this method may be more useful for this specific application and testing is ongoing.

Gene transfection using commercial PEI preparations is also effective (Fig. 4). Our results complement those of an earlier study [42] that successfully used the PEI method to deliver the dopamine transporter gene to cells of the SN. Taken together, the results show that PEI transfection does work, although the efficacy of gene delivery varies from experiment to experiment, which could reflect differences between the batches of polymer or difficulty in controlling experimental variables. In addition, this method was significantly less effective than a recently reported brain gene transfer using organically modified silica nanoparticles [18]. Further improvements in PEI method are thus required. We used the 22 kDa PEI, since it was reported that the small size PEIs appear to be superior to the larger size molecules in gene transfection [34, 35]. Since it has been reported that low molecular weight PEI's, 0.5–10 kDa made by fractionating commercially available 25 kDa PEI, were shown to have a better rate of transfection and were less cytotoxic than the unfractionated 25 kDa PEI by itself [3], future improvements will take these ideas into account as well as others, such as a report showing the increasing effectiveness of DNA/PEI delivery using a slow release delivery system that delivers DNA/PEI complexes for several days [52]. There are several reports demonstrating chemical modifications of PEI's have been shown superior transfection over the non-modified PEI's [2, 30, 43, 60, 73, 74]. Another concern deals with studies by others on the mechanism of PEI gene delivery, indicating that a relatively small fraction of DNA/PEI complexes reach the nucleus [4].

In the present study, the non-replicating HSV-1 8117/43 construct, in which the *lacZ* gene is driven by combined LAT and MoMuLV LTR promoters, gave the strongest signal following delivery of this reporter

gene (Fig. 1). This complements other studies, which use this vector as a delivery vehicle to a number of distinct sites within CNS [6, 59], specifically SN [40] and hippocampus [7]. Early reports with HSV vectors have showed decreased reporter gene expression during latent infection with HSV LAT promoter constructs [41]. However, introduction of the tandem MoMuLV LTR/LAT promoters increased the efficiency and duration of reporter gene expression [7, 37].

For HSV-1 8117/43 the length of expression and the number of cells expressing the reporter gene are both significant and useful, more for acute basic applications. These may include *in vivo* intracerebral gene transfer to investigate underlying mechanisms and potential corrective therapies for neurodegenerative diseases, especially those involving the nigrostriatal pathway.

Another promising development has been the construction of the amplicon HSV-1 vector. Although the effect observed with this vector (Fig. 2) was not as robust as the 8117/43 HSV-1 (Fig. 1), it is important to note that the 8117/43 HSV-1 could be inoculated at a titer approximately 10 times higher than the amplicon virus as a result of its ability to be produced at higher titers without a helper virus. However, the efficacy of gene expression of the amplicon was significantly enhanced when used with a helper virus (Fig. 2, panels I, II and III). Thus, in biological experiments in which maximally effective gene delivery is essential, it may be advantageous to use a helper virus containing amplicon preparations.

The use of the amplicon to deliver FGFR1(TK-) showed a highly reproducible effect from one animal to the next [17]. Cell counts of all TH-positive cells in SN of rats injected on only one side of the brain showed a significant decrease on FGFR1(TK-) side compared to the non-injected side [17]. There was no significant difference between the numbers of TH-positive cells on the  $\beta$ -galactosidase injected side compared to its non-injected side. A comparison of the  $\beta$ -galactosidase injected rats compared to FGFR(TK-) rats showed a decrease in the number of cells [17]. A similar decrease was observed with PEI-transfected FGFR1(TK-), although these results were not statistically significant because of the great individual variation within groups.

Another outcome of this study was that HSV-1 vectors expressed the transgene exclusively in neuronal like cells, whereas PEI expressed the transgene both in neurons and in glial cells (Fig. 4). Hence non-viral methods may be advantageous when gene transfer to different types of brain cell is required.

This finding is consistent with the tenet that viral transfected cells (recombinant adeno-associated virus-2) were mostly neurons, where the non-viral methods tended to target both neurons and glia [26]. Given that HSV-1 infections, which appeared to be exclusively neuronal, had a similar effect on TH neurons as PEI transfection, it is likely that the effects of FGFR1(TK-) were produced directly in SN neurons. We have further found (Table 1) that the cells on the virus-injected side might be slightly larger, although the increase is not statistically convincing.

Our interest in this work stems from the fact that progress in treating diseases like PD is hampered by the lack of animal models that mimic progressive and specific degeneration of the dopaminergic (DA) neurons of SN, as well as by an insufficient understanding of the mechanisms leading to neuronal death. Since there are rare familial cases of PD associated with mutations in the *synuclein* or the *parkin* genes [25, 31, 32], we have an interest in other gene malfunctions that could play a role in PD.

In summary, both viral and non-viral methods are effective in introducing functional recombinant genes into CNS. These methods should be further developed to improve their efficacy and reduce potential tissue damaging effects. These methods may be a valuable alternative to transgenic animals in developing new disease models and testing new therapeutic approaches.

## ACKNOWLEDGEMENTS

We thank students Lawrence C. Jenkins and Marghuretta Bland for assisting in surgical and histological procedures and Ann Casey in preparation of the HSV amplicon vector stocks. This study was supported by NIH NS43621-01 and NSF IBN-9728923. Students participating in this study were supported by NSF Undergraduate Research Experience supplement (C.G.) and by Canisius College Earning Excellence Program (A.S.G, T.B. and J.N.).

## REFERENCES

1. Abdallah B, Hassan A, Benoist C, Goula D, Behr JP, Demeneix BA (1996) A powerful nonviral vector for *in vivo* gene transfer into the adult mammalian brain: polyethylenimine. *Hum Gene Ther*, 7: 1947-1954.
2. Bettinger T, Remy JS, Erbacher P (1999) Size reduction of galactosylated PEI/DNA complexes improves lectin-mediated gene transfer into hepatocytes. *Bioconjug Chem*, 10: 558-561.
3. Bieber T, Elsasser HP (2001) Preparation of a low molecular weight polyethylenimine for efficient cell transfection. *Biotechniques*, 30: 74-77, 80-81.

4. Bieber T, Meissner W, Kostin S, Niemann A, Elsasser HP (2002) Intracellular route and transcriptional competence of polyethylenimine-DNA complexes. *J Control Release*, 82: 441–454.
5. Bisht S, Bhakta G, Mitra S, Maitra A (2005) pDNA loaded calcium phosphate nanoparticles: highly efficient non-viral vector for gene delivery. *Int J Pharm*, 288: 157–168.
6. Bloom DC, Jarman RG (1998) Generation and use of recombinant reporter viruses for study of herpes simplex virus infections *in vivo*. *Methods*, 16: 117–125.
7. Bloom DC, Maidment NT, Tan A, Dissette VB, Feldman LT, Stevens JG (1995) Long-term expression of a reporter gene from latent herpes simplex virus in the rat hippocampus. *Brain Res Mol Brain Res*, 31: 48–60.
8. Boussif O, Lezoualch F, Zanta MA, Mergny MD, Scherman D, Demeneix B, Behr JP (1995) A versatile vector for gene and oligonucleotide transfer into cells in culture and *in vivo*: polyethylenimine. *Proc Natl Acad Sci USA*, 92: 7297–7301.
9. Bowers WJ, Chen X, Guo H, Frisina DR, Federoff HJ, Frisina RD (2002) Neurotrophin-3 transduction attenuates cisplatin spiral ganglion neuron ototoxicity in the cochlea. *Mol Ther*, 6: 12–18.
10. Bowers WJ, Howard DF, Brooks AI, Halterman MW, Federoff HJ (2001) Expression of vhs and VP16 during HSV-1 helper virus-free amplicon packaging enhances titers. *Gene Ther*, 8: 111–120.
11. Bowers WJ, Howard DF, Federoff HJ (2000) Discordance between expression and genome transfer titering of HSV amplicon vectors: recommendation for standardized enumeration. *Mol Ther*, 1: 294–299.
12. Bowers WJ, Olschowka JA, Federoff HJ (2003) Immune responses to replication-defective HSV-1 type vectors within the CNS: implications for gene therapy. *Gene Ther*, 10: 941–945.
13. Brooks AI, Cory-Slechta DA, Bowers WJ, Murg SL, Federoff HJ (2000) Enhanced learning in mice parallels vector-mediated nerve growth factor expression in hippocampus. *Hum Gene Ther*, 11: 2341–2352.
14. Chen X, Frisina RD, Bowers WJ, Frisina DR, Federoff HJ (2001) HSV amplicon-mediated neurotrophin-3 expression protects murine spiral ganglion neurons from cisplatin-induced damage. *Mol Ther*, 3: 958–963.
15. Coll JL, Chollet P, Brambilla E, Desplanques D, Behr JP, Favrot M (1999) *In vivo* delivery to tumors of DNA complexed with linear polyethylenimine. *Hum Gene Ther*, 10: 1659–1666.
16. Corso T, Torres G, Goulah C, Roy I, Gambino A, Nayda J, Buckley T, Stachowiak E, Bergery E, Pudavar H, Dutta P, Bloom D, Bowers W, Stachowiak M (2005) Transfection of tyrosine kinase deleted FGF receptor-1 into rat brain substantia nigra reduces the number of tyrosine hydroxylase expressing neurons and decreases concentration levels of striatal dopamine. *J Mol Brain Res* (in press).
17. Corso TD, Torres G, Goulah C, Roy I, Gambino AS, Nayda J, Buckley T, Stachowiak EK, Bergery EJ, Pudavar H, Dutta P, Bloom DC, Bowers WJ, Stachowiak MK (2005) Transfection of tyrosine kinase deleted FGF receptor-1 into rat brain substantia nigra reduces the number of tyrosine hydroxylase expressing neurons and decreases concentration levels of striatal dopamine. *Mol Brain Res* (in press).
18. Bharali DJ, Klejbor I, Stachowiak EK, Dutta P, Roy I, Kaur N, Bergery EJ, Prasad PN, Stachowiak MK (2005) Organically modified silica nanoparticles a novel non-viral vector for *in vivo* gene delivery and expression in the brain. *Proceedings of the National Academy of Science, USA* (in press).
19. Dobson AT, Margolis TP, Sedarati F, Stevens JG, Feldman LT (1990) A latent, nonpathogenic HSV-1-derived vector stably expresses beta-galactosidase in mouse neurons. *Neuron*, 5: 353–360.
20. Gallot D, Seifer I, Lemery D, Bignon YJ (2002) Systemic diffusion including germ cells after plasmidic *in utero* gene transfer in the rat. *Fetal Diagn Ther*, 17: 157–162.
21. Geller AI, Breakefield XO (1988) A defective HSV-1 vector expresses *Escherichia coli* beta-galactosidase in cultured peripheral neurons. *Science*, 241: 1667–1669.
22. Goula D, Remy JS, Erbacher P, Wasowicz M, Levi G, Abdallah B, Demeneix BA (1998) Size, diffusibility and transfection performance of linear PEI/DNA complexes in the mouse central nervous system. *Gene Ther*, 5: 712–717.
23. Graham FL, van der Eb AJ (1973) A new technique for the assay of infectivity of human adenovirus 5 DNA. *Virology*, 52: 456–467.
24. Halaby IA, Lyden SP, Davies MG, Roztocil E, Salamone LJ, Brooks AI, Green RM, Federoff HJ, Bowers WJ (2002) Glucocorticoid-regulated VEGF expression in ischemic skeletal muscle. *Mol Ther*, 5: 300–306.
25. Hattori N, Kitada T, Matsumine H, Asakawa S, Yamamura Y, Yoshino H, Kobayashi T, Yokochi M, Wang M, Yoritaka A, Kondo T, Kuzuhara S, Nakamura S, Shimizu N, Mizuno Y (1998) Molecular genetic analysis of a novel Parkin gene in Japanese families with autosomal recessive juvenile parkinsonism: evidence for variable homozygous deletions in the Parkin gene in affected individuals. *Ann Neurol*, 44: 935–941.
26. Hirko AC, Bueth DD, Meyer EM, Hughes JA (2002) Plasmid delivery in the rat brain. *Biosci Rep*, 22: 297–308.
27. Hocknell PK, Wiley RD, Wang X, Evans TG, Bowers WJ, Hanke T, Federoff HJ, Dewhurst S (2002) Expression of human immunodeficiency virus type 1 gp120 from herpes simplex virus type 1-derived amplicons results in potent, specific, and durable cellular and humoral immune responses. *J Virol*, 76: 5565–5580.
28. Horbinski C, Stachowiak EK, Chandrasekaran V, Miuzukoshi E, Higgins D, Stachowiak MK (2002) Bone morphogenetic protein-7 stimulates initial dendritic growth in sympathetic neurons through an intracellular fibroblast growth factor signaling pathway. *J Neurochem*, 80: 54–63.
29. Horbinski C, Stachowiak MK, Higgins D, Finnegan SG (2001) Polyethyleneimine-mediated transfection of cultured postmitotic neurons from rat sympathetic ganglia and adult human retina. *BMC Neurosci*, 2: 2.
30. Kichler A, Chillon M, Leborgne C, Danos O, Frisch B (2002) Intranasal gene delivery with a polyethyleneimine-PEG conjugate. *J Control Release*, 81: 379–388.
31. Kitada S, Kojima K, Shimokata K, Ogishima T, Ito A (1998) Glutamate residues required for substrate binding and cleavage activity in mitochondrial processing peptidase. *J Biol Chem*, 273: 32547–32553.

32. Kitada T, Asakawa S, Hattori N, Matsumine H, Yamamura Y, Minoshima S, Yokochi M, Mizuno Y, Shimizu N (1998) Mutations in the parkin gene cause autosomal recessive juvenile parkinsonism. *Nature*, 392: 605–608.
33. Kofler P, Wiesenhofer B, Rehl C, Baier G, Stockhammer G, Humpel C (1998) Liposome-mediated gene transfer into established CNS cell lines, primary glial cells, and *in vivo*. *Cell Transplant*, 7: 175–185.
34. Kunath K, von Harpe A, Fischer D, Petersen H, Bickel U, Voigt K, Kissel T (2003) Low-molecular-weight polyethylenimine as a non-viral vector for DNA delivery: comparison of physicochemical properties, transfection efficiency and *in vivo* distribution with high-molecular-weight polyethylenimine. *J Control Release*, 89: 113–125.
35. Lemkine GF, Demeneix BA (2001) Polyethylenimines for *in vivo* gene delivery. *Curr Opin Mol Ther*, 3: 178–182.
36. Lemkine GF, Mantero S, Migne C, Raji A, Goula D, Normandie P, Levi G, Demeneix BA (2002) Preferential transfection of adult mouse neural stem cells and their immediate progeny *in vivo* with polyethylenimine. *Mol Cell Neurosci*, 19: 165–174.
37. Lokensgard JR, Bloom DC, Dobson AT, Feldman LT (1994) Long-term promoter activity during herpes simplex virus latency. *J Virol*, 68: 7148–7158.
38. Lu B, Gupta S, Federoff H (1995) *Ex vivo* hepatic gene transfer in mouse using a defective herpes simplex virus-1 vector. *Hepatology*, 21: 752–759.
39. Maguir-Zeis KA, Bowers WJ, Federoff HJ (2001) HSV vector-mediated gene delivery to the central nervous system. *Curr Opin Mol Ther*, 3: 482–490.
40. Maidment NT, Tan AM, Bloom DC, Anton B, Feldman LT, Stevens JG (1996) Expression of the lacZ reporter gene in the rat basal forebrain, hippocampus, and nigrostriatal pathway using a nonreplicating herpes simplex vector. *Exp Neurol*, 139: 107–114.
41. Margolis TP, Bloom DC, Dobson AT, Feldman LT, Stevens JG (1993) Decreased reporter gene expression during latent infection with HSV LAT promoter constructs. *Virology*, 197: 585–592.
42. Martres MP, Demeneix B, Hanoun N, Hamon M, Giros B (1998) Up- and down-expression of the dopamine transporter by plasmid DNA transfer in the rat brain. *Eur J Neurosci*, 10: 3607–3616.
43. Morimoto K, Nishikawa M, Kawakami S, Nakano T, Hattori Y, Fumoto S, Yamashita F, Hashida M (2003) Molecular weight-dependent gene transfection activity of unmodified and galactosylated polyethylenimine on hepatoma cells and mouse liver. *Mol Ther*, 7: 254–261.
44. Olschowka JA, Bowers WJ, Hurley SD, Mastrangelo MA, Federoff HJ (2003) Helper-free HSV-1 amplicons elicit a markedly less robust innate immune response in the CNS. *Mol Ther*, 7: 218–227.
45. Ouatas T, Le Mevel S, Demeneix BA, de Luze A (1998) T3-dependent physiological regulation of transcription in the *Xenopus tadpole* brain studied by polyethylenimine based *in vivo* gene transfer. *Int J Dev Biol*, 42: 1159–1164.
46. Paterson T, Everett RD (1990) A prominent serine-rich region in Vmw175, the major transcriptional regulator protein of herpes simplex virus type 1, is not essential for virus growth in tissue culture. *J Gen Virol*, 71 (Pt 8): 1775–1783.
47. Paxinos G, Watson C (1998) *The Rat Brain in Stereotaxic Coordinates*. 4<sup>th</sup> Ed. Academic Press.
48. Peng H, Moffett J, Myers J, Fang X, Stachowiak EK, Maher P, Kratz E, Hines J, Fluharty SJ, Mizukoshi E, Bloom DC, Stachowiak MK (2001) Novel nuclear signaling pathway mediates activation of fibroblast growth factor-2 gene by type 1 and type 2 angiotensin II receptors. *Mol Biol Cell*, 12: 449–462.
49. Peng H, Myers J, Fang X, Stachowiak EK, Maher PA, Martins GG, Popescu G, Berezney R, Stachowiak MK (2002) Integrative nuclear FGFR1 signaling (INFS) pathway mediates activation of the tyrosine hydroxylase gene by angiotensin II, depolarization and protein kinase C. *J Neurochem*, 81: 506–524.
50. Roessler BJ, Davidson BL (1994) Direct plasmid mediated transfection of adult murine brain cells *in vivo* using cationic liposomes. *Neurosci Lett*, 167: 5–10.
51. Roy I, Mitra S, Maitra A, Mozumdar S (2003) Calcium phosphate nanoparticles as novel non-viral vectors for targeted gene delivery. *Int J Pharm*, 250: 25–33.
52. Scherer F, Schillinger U, Putz U, Stemberger A, Plank C (2002) Nonviral vector loaded collagen sponges for sustained gene delivery *in vitro* and *in vivo*. *J Gene Med*, 4: 634–643.
53. Sedarati F, Margolis TP, Stevens JG (1993) Latent infection can be established with drastically restricted transcription and replication of the HSV-1 genome. *Virology*, 192: 687–691.
54. Stachowiak EK, Fang X, Myers J, Dunham S, Stachowiak MK (2003) cAMP-induced differentiation of human neuronal progenitor cells is mediated by nuclear fibroblast growth factor receptor-1 (FGFR1). *J Neurochem*, 84: 1296–1312.
55. Stachowiak EK, Maher PA, Tucholski J, Mordechai E, Joy A, Moffett J, Coons S, Stachowiak MK (1997) Nuclear accumulation of fibroblast growth factor receptors in human glial cells-association with cell proliferation. *Oncogene*, 14: 2201–2211.
56. Stachowiak MK, Maher PA, Joy A, Mordechai E, Stachowiak EK (1996) Nuclear accumulation of fibroblast growth factor receptors is regulated by multiple signals in adrenal medullary cells. *Mol Biol Cell*, 7: 1299–1317.
57. Stavropoulos TA, Strathdee CA (1998) An enhanced packaging system for helper-dependent herpes simplex virus vectors. *J Virol*, 72: 7137–7143.
58. Stevens JG (1989) Human herpesviruses: a consideration of the latent state. *Microbiol Rev*, 53: 318–332.
59. Tabbas S, Goulah C, Tran RK, Lis A, Korody R, Stachowski B, Horowitz JM, Torres G, Stachowiak EK, Bloom DC, Stachowiak MK (2000) Gene transfer into the central nervous system using herpes simplex virus-1 vectors. *Folia Morphol (Warsz)*, 59: 221–232.
60. Tang GP, Zeng JM, Gao SJ, Ma YX, Shi L, Li Y, Too HP, Wang S (2003) Polyethylene glycol modified polyethylenimine for improved CNS gene transfer: effects of PEGylation extent. *Biomaterials*, 24: 2351–2362.
61. Tolba KA, Bowers WJ, Eling DJ, Casey AE, Kipps TJ, Federoff HJ, Rosenblatt JD (2002) HSV amplicon-

- mediated delivery of LIGHT enhances the antigen-presenting capacity of chronic lymphocytic leukemia. *Mol Ther*, 6: 455–463.
62. Tolba KA, Bowers WJ, Hilchey SP, Halterman MW, Howard DF, Giuliano RE, Federoff HJ, Rosenblatt JD (2001) Development of herpes simplex virus-1 amplicon-based immunotherapy for chronic lymphocytic leukemia. *Blood*, 98: 287–295.
  63. Tolba KA, Bowers WJ, Muller J, Houseknecht V, Giuliano RE, Federoff HJ, Rosenblatt JD (2002) Herpes simplex virus (HSV) amplicon-mediated codelivery of secondary lymphoid tissue chemokine and CD40L results in augmented antitumor activity. *Cancer Res*, 62: 6545–6551.
  64. Tooyama I, Kawamata T, Walker D, Yamada T, Hanai K, Kimura H, Iwane M, Igarashi K, McGeer EG, McGeer PL (1993) Loss of basic fibroblast growth factor in substantia nigra neurons in Parkinson's disease. *Neurology*, 43: 372–376.
  65. Tooyama I, McGeer EG, Kawamata T, Kimura H, McGeer PL (1994) Retention of basic fibroblast growth factor immunoreactivity in dopaminergic neurons of the substantia nigra during normal aging in humans contrasts with loss in Parkinson's disease. *Brain Res*, 656: 165–168.
  66. Truong-Le VL, Walsh SM, Schweibert E, Mao HQ, Guggino WB, August JT, Leong KW (1999) Gene transfer by DNA-gelatin nanospheres. *Arch Biochem Biophys*, 361: 47–56.
  67. Ueno H, Gunn M, Dell K, Tseng A Jr, Williams L (1992) A truncated form of fibroblast growth factor receptor 1 inhibits signal transduction by multiple types of fibroblast growth factor receptor. *J Biol Chem*, 267: 1470–1476.
  68. Wagner EK, Bloom DC (1997) Experimental investigation of herpes simplex virus latency. *Clin Microbiol Rev*, 10: 419–443.
  69. Walker DG, Terai K, Matsuo A, Beach TG, McGeer EG, McGeer PL (1998) Immunohistochemical analyses of fibroblast growth factor receptor-1 in the human substantia nigra. Comparison between normal and Parkinson's disease cases. *Brain Res*, 794: 181–187.
  70. Wang X, Wiley RD, Evans TG, Bowers WJ, Federoff HJ, Dewhurst S (2003) Cellular immune responses to helper-free HSV-1 amplicon particles encoding HIV-1 gp120 are enhanced by DNA priming. *Vaccine*, 21: 2288–2297.
  71. Wightman L, Kircheis R, Rossler V, Carotta S, Ruzicka R, Kursa M, Wagner E (2001) Different behavior of branched and linear polyethylenimine for gene delivery *in vitro* and *in vivo*. *J Gene Med*, 3: 362–372.
  72. Willis RA, Bowers WJ, Turner MJ, Fisher TL, Abdul-Alim CS, Howard DF, Federoff HJ, Lord EM, Frelinger JG (2001) Dendritic cells transduced with HSV-1 amplicons expressing prostate-specific antigen generate antitumor immunity in mice. *Hum Gene Ther*, 12: 1867–1879.
  73. Yamazaki Y, Nango M, Matsuura M, Hasegawa Y, Hasegawa M, Oku N (2000) Polycation liposomes, a novel nonviral gene transfer system, constructed from cetylated polyethylenimine. *Gene Ther*, 7: 1148–1155.
  74. Zanta MA, Boussif O, Adib A, Behr JP (1997) *In vitro* gene delivery to hepatocytes with galactosylated polyethylenimine. *Bioconjug Chem*, 8: 839–844.